Available online at www.sciencedirect.com
ScienceDirect
C. R. Mecanique 334 (2006) 493–506
COMPTES RENDUS MECANIQUE
http://france.elsevier.com/direct/CRAS2B/

Observation, analysis and modelling in complex fluid media

Dissipation element analysis of scalar fields in turbulence

Norbert Peters *, Lipo Wang

Institut für Technische Verbrennung, RWTH-Aachen, Templergraben 64, 52064 Aachen, Germany

Available online 6 September 2006

Abstract

The field of the fluctuating scalar obtained from Direct Numerical Simulation (DNS) in homogeneous shear flow is subdivided into finite size regions within which it varies monotonously. These regions are called dissipation elements and are identified by calculating trajectories normal to isoscalar surfaces starting from every grid point until a minimum and a maximum point is reached. Two parameters describe the statistical properties of dissipation elements sufficiently well: the linear distance between the minimum and maximum points and the absolute value of the scalar difference at these points. The joint probability density function of these parameters decomposes into a conditional pdf of the scalar difference and the marginal pdf of the distance between the minimum and maximum points, the latter being the object of this study.

For the length scale distribution function a stochastic evolution equation was derived in a companion paper. It implies the cutting and reconnection of linear elements and the effect of molecular diffusion. The equation is an integral equation and must be solved numerically. In this paper we show how one-dimensional simulations of randomly generated scalar profiles would illustrate the cutting and reconnection processes as well as the drift and disappearance of small elements by molecular diffusion. The resulting distribution function from the simulation shows good agreement with the predicted distribution function. It is concluded that the mean distance between extremal points is of the order of the scalar Taylor length. ***To cite this article: N. Peters, L. Wang, C. R. Mecanique 334 (2006).***

Résumé

Analyse d'éléments de dissipation de champs scalaires turbulents. Le champ d'un scalaire fluctuant obtenu par Simulation Numérique Directe (DNS) dans un écoulement cisaillé homogène est subdivisé en régions de taille finie dans lesquelles il varie de manière monotone. Ces régions sont appelées éléments de dissipation et sont identifiées par calcul des trajectoires normales aux surfaces iso-scalaires à partir de chaque point de grille jusqu'à ce que des points minimum et maximum soient atteints. Deux paramètres décrivent les propriétés statistiques des éléments de dissipation assez bien : la distance linéaire entre les points maximum et minimum et la valeur absolue de la différence scalaire en ces points. La fonction densité de probabilité conjointe de ces paramètres se décompose en une fonction densité de probabilité conditionnelle de la différence scalaire et de la fonction densité de probabilité marginale de la distance entre les points minimum et maximum, ce dernier étant l'objet de cette étude.

Pour la fonction distribution d'échelles de longueur, une équation d'évolution stochastique à été obtenue dans un précédent papier. Ceci implique la coupure et la reconnection d'éléments linéaires et l'effet de la diffusion moléculaire. L'équation est une équation intégrale qui doit être résolue numériquement. Dans ce papier nous montrons comment des simulations unidimensionnelle de profils scalaires générés aléatoirement pourraient illustrer les processus de coupure et de reconnection ainsi que la dérive et la disparition de petits éléments par diffusion moléculaire. La fonction distribution obtenue à partir de la simulation montre un bon

* Corresponding author.
E-mail addresses: N.Peters@ITV.RWTH-Aachen.de (N. Peters), L.Wang@ITV.RWTH-Aachen.de (L. Wang).

1631-0721/$ – see front matter
doi:10.1016/j.crme.2006.07.006

accord avec la fonction distribution prédite. On en conclut que la distance moyenne entre points extrêmes est de l'ordre de l'échelle de Taylor. ***Pour citer cet article : N. Peters, L. Wang, C. R. Mecanique 334 (2006).***

Keywords: Turbulence; Passive scalar mixing; Length scales; Dissipation element

Mots-clés : Turbulence ; Mélange d'un scalaire passif ; Échelles de longueur ; Éléments de dissipation

1. Introduction

In search for random geometrical elements in turbulence that would represent turbulent 'eddies', one realizes that there is a need to subdivide the flow into finite size regions. The subdivision should not be arbitrary as by a numerical mesh but should follow from the structures of the flow itself. Useful corner points would be singular points that the flow itself generates, and the boundaries of the elements should be related to physical processes that one recognizes as being important. Such a process is viscous dissipation of kinetic energy, or since here we are interested in passive scalars, scalar dissipation. If one imagines, for simplicity, a one-dimensional profile of a passive scalar ϕ, as shown in Fig. 1, one can identify local minimum and maximum points, and subdivide the profile into elements between these points, each having a finite length l_i and a scalar difference $\Delta\phi_i$. Since this profile is subjected to diffusion due to the nature of the diffusion equation, local minima and maxima values of ϕ would move towards the large time mean value of the scalar, which is equivalent to scalar dissipation. Therefore the finite elements extending between minimum and maximum points will be called dissipation elements.

Dissipation elements can also be identified in two- or three-dimensional scalar fields. A scalar can be any scalar quantity such as the components of the velocity field or simply a passive scalar. The latter is the object of the present study. For simplicity again, imagine a two-dimensional passive scalar field with minimum and maximum points randomly distributed over space. This is shown schematically in Fig. 2 together with some isoscalar lines around these extremal points and geodetic lines that connect two maxima or minima and pass through a saddle points. The saddle points represent relative minima on the ridge lines and relative maxima along the geodetic lines that connect two minima. It is evident that along these lines the scalar gradient in normal direction vanishes. Four repeating units covering a finite spatial region between the central minimum point and four different maximum points are shown in Fig. 2. They are bounded by zero normal gradient lines which connect the extremal points through saddle points.

If the scalar field in two or three dimensions is known at a fixed time t, for instance from Direct Numerical Simulations (DNS), trajectories can be calculated that start from any point within the elements in direction of both ascending and descending scalar gradients. Such a trajectory, also shown in the upper right dissipation element in

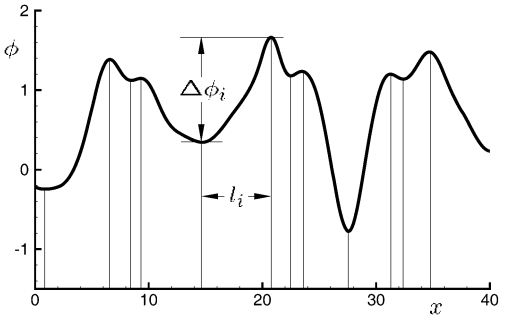

Fig. 1. The parameters of a dissipation element: linear distance l_i and absolute value of the scalar difference $\Delta\phi_i$.

Fig. 1. Paramètres d'un élément de dissipation : distance linéaire l_i et valeur absolue de la différence scalaire $\Delta\phi_i$.

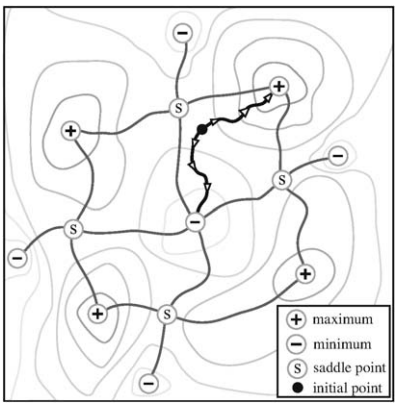

Fig. 2. Schematic sketch of a 2D scalar field including the trajectory from an initial point to the minimum and maximum points.

Fig. 2. Vue schématique d'un champ scalaire 2D incluant la trajectoire d'un point initial aux points maximum et minimum.

Fig. 1, would inevitably reach the minimum and the maximum points. Since it cannot leave the element which is bounded by zero normal gradient lines (in 2D) or zero normal surfaces (in 3D) the spatial domain of the dissipation element extends over the ensemble of grid points within it. We will assume that the scalar field is sufficiently smooth to satisfy the conditions of a Morse function which takes a pure quadratic form in the vicinity of the extremal points.

Carl Gibson [1] was the first to analyze in detail the properties of zero-gradient points and minimal gradient surfaces in passive scalar turbulence with a mean scalar gradient. He pointed out that in 1D the number of minimum and maximum points should be equal; in 2D the sum of those two numbers should be equal to the number of saddle points, as it is evident from Fig. 2. In 3D, the topology is much more complicated.

Gibson [1] also analyzed the mechanism by which extremal points are generated. He notes that in the absence of diffusion convective motion alone is unable to generate extremal points, because isoscalar surfaces will just follow the fluid motion even if this leads to very large distortions of these surfaces (as one observes in high Prandtl number flows, for instance). Only a diffusion velocity of the same magnitude as the local convective velocity is able to restore the isoscalar surfaces and to generate extremal points. The analysis shows that in scalar turbulence the local convective velocity is of the order of the Kolmogorov velocity $v_K = (\varepsilon r)^{1/3}$ while the balancing diffusive velocity is $v_C = D/r$. Equating these two velocities, Gibson finds that extremal points are generated at scales of the Obukhov–Corrsin length

$$L_C = \left(\frac{D^3}{\varepsilon}\right)^{1/4} \tag{1}$$

and that there may be secondary splitting of extremal points by local strain. According to this theory the generation of extremal points occurs randomly by eddy turnover of small scale eddies. The frequency at which this occurs, however, is yet unknown.

In this article we will formulate a one-dimensional stochastic model that mimics the generation of extremal points, but also its disappearance by diffusion. We will compare the resulting length scale probability density function and properties with a predicted formulation from a companion paper. This will resolve the question about the frequency, at which extremal points are randomly generated.

2. Dissipation elements obtained from Direct Numerical Simulation

We have performed DNS simulations of turbulent homogeneous shear flow on a 128^3 spatial grid in a cube of side 2π. The field of a passive scalar was also calculated for a unity Prandtl number.

A mean scalar gradient S_ϕ was imposed which was in the same x_2-direction as the velocity gradient. Apart from the viscosity $\nu = 0.01$, the shear rate $S = \partial\langle u_1\rangle/\partial x_2 = 1.0$ and $S_\phi = \partial\langle\phi\rangle/\partial x_2 = 1/(2\pi)$ the initial turbulent kinetic energy $k_0 = 2.0$ and its initial dissipation $\varepsilon_0 = 4.0$ were prescribed. This determines the initial eddy turnover time as $t_0 = k_0/\varepsilon_0 = 0.5$. The code is an incompressible version of the spectral code by Sarker [2].

As examples, in Fig. 3 two dissipation elements are shown by their trajectories between the minimum point (blue) and the maximum point (red). They were obtained after 80 initial eddy turnover times when the turbulent kinetic energy k, after having fallen to a value of $k = 0.12$, was increasing again due to production by shear. It then had reached a value of $k = 2.0$, whereas the dissipation was $\varepsilon = 0.9$. The scalar variance was $\langle\phi'^2\rangle = 0.039$ and the mean scalar dissipation rate $\chi = 0.0388$. The elements are quite irregular and sometimes flat near one extremal point having a sharp edge at the other. In Wang and Peters [3] the average shape of the elements was calculated. They can be viewed, on average, as one-dimensional rods with a diameter of a few Kolmogorov scales but with a largely varying length. There were approximately 6000 dissipation elements in the 128^3 cube.

Among the many parameters that would potentially describe the statistical properties of those dissipation elements, we have chosen the linear distance between the minimum and maximum points and the absolute scalar difference at these points. A third parameter to be used in future studies is the algebraic mean of the scalar difference. Fig. 4 shows, again as an example, the joint pdf of the scalar difference $\Delta\phi' = |\phi'(\mathbf{x}_{\min}) - \phi'(\mathbf{x}_{\max})|$ and the linear distance $l = |\mathbf{x}_{\max} - \mathbf{x}_{\min}|$, where $\phi' = \phi(\mathbf{x}) - x_2 S_\phi$ is the scalar fluctuation. It was obtained by evaluating 20 consecutive scalar fields at a time interval of 0.2 eddy turnover times, for the last 4 eddy turnover times of the simulation described

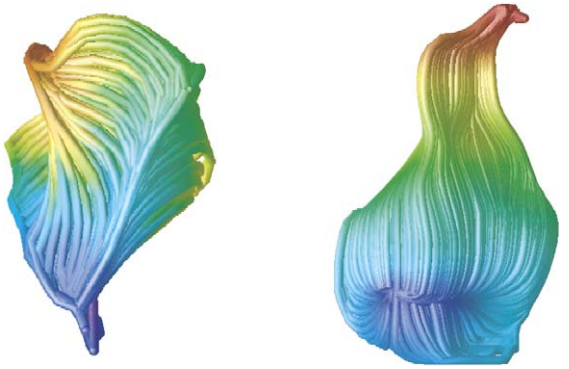

Fig. 3. The shape of two dissipation elements calculated from trajectories.

Fig. 3. Formes de deux élément de dissipation calculées à partir des trajectoires.

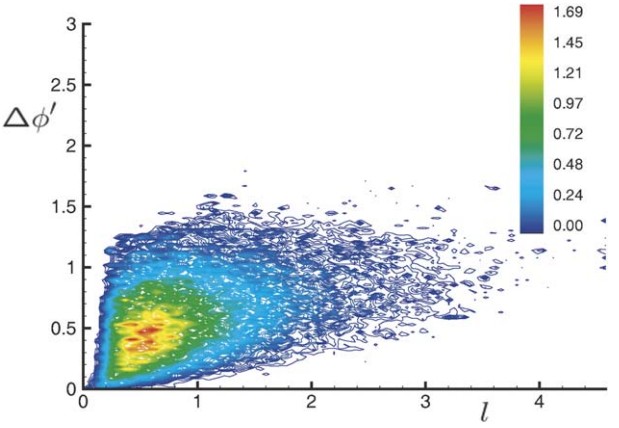

Fig. 4. Joint pdf of the scalar difference and the element length scale.

Fig. 4. Fonction densité de probabilité conjointe de la différence scalaire et de l'échelle de longueur de l'élément.

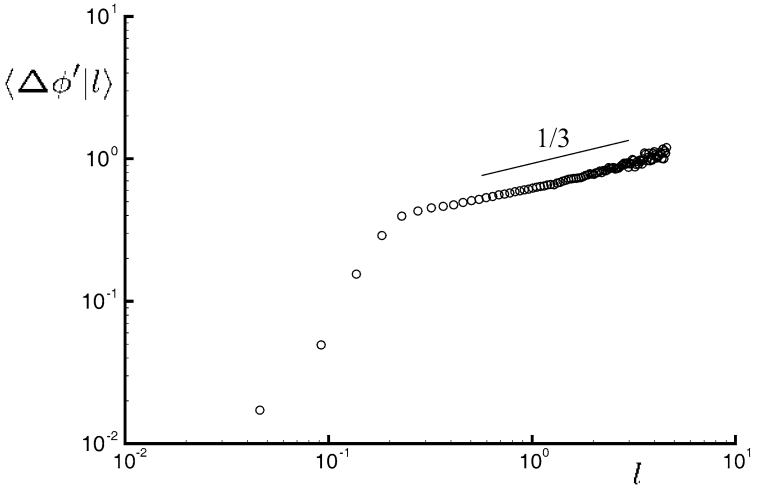

Fig. 5. Scaling of the conditional mean scalar difference.

Fig. 5. Loi déchelle de la moyenne conditionnelle de la différence scalaire.

above. According to Bayes' theorem the joint pdf $P(\Delta\phi', l)$ can be written as the product of the conditional pdf of the scalar difference $P_{\Delta\phi'}(\Delta\phi'|l)$ and the marginal pdf $P_l(l)$

$$P(\Delta\phi', l) = P_{\Delta\phi'}(\Delta\phi'|l)\,P_l(l) \tag{2}$$

where

$$P_l(l) = \int_0^\infty P(\Delta\phi', l)\,\mathrm{d}(\Delta\phi') \tag{3}$$

It is interesting to note that the conditional mean $\langle \Delta\phi'|l \rangle$ defined by

$$\langle \Delta\phi'|l \rangle = \int_0^\infty (\Delta\phi')\,P_{\Delta\phi'}(\Delta\phi'|l)\,\mathrm{d}(\Delta\phi') \tag{4}$$

follows the Kolmogorov $l^{1/3}$ scaling for the large scales as shown in Fig. 5.

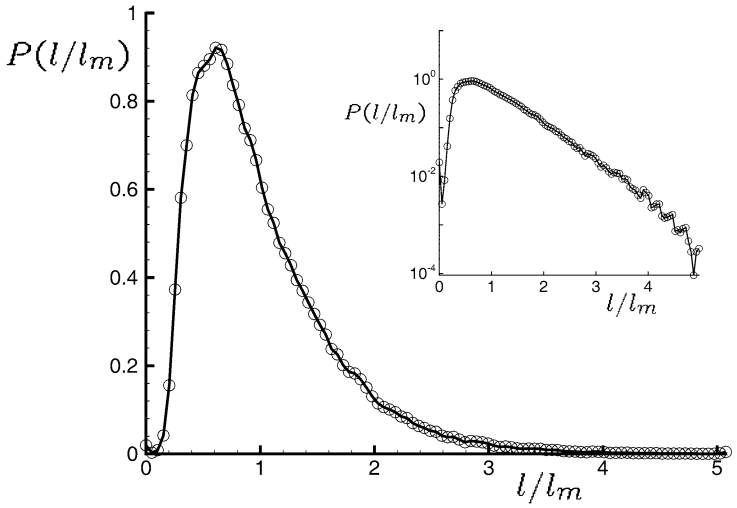

Fig. 6. Normalized length scale distribution from 3D DNS.

Fig. 6. Distribution normalisée de l'échelle scalaire à partir de DNS 3D.

Fig. 6 shows the marginal pdf $P_l(l)$ calculated from (3). Both the pdf and the element length have been normalized by the mean length scale l_m. It is seen to have a maximum at $l/l_m = 0.6$ where $P_l(l/l_m) = 0.92$. The inserted log-linear graph in Fig. 6 shows that the pdf decays exponentially for large values of l. The mean length scale $l_m = 0.9$ needs to be compared to the Kolmogorov and the Obukhov–Corrsin scales which are both equal to 0.03, and to the Taylor scale $\lambda = 0.47$, as well as the integral scale $l_t = k^{3/2}/\varepsilon = 3.14$.

Since for this DNS the Taylor Reynolds number of 54 is still relatively small, it would be difficult to draw a conclusion about the nature of the mean length scale at this point.

3. Theory

We are interested in the probability density of elements with length l. This length is the linear distance between the extremal points. Following Carl Gibson's analysis we postulate that the time evolution of extremal points exhibits several stochastic features:

(1) The generation of new extremal points resulting from random eddy turnover of Obukhov–Corrsin eddies. This will be called the cutting process.
(2) The merging of two extremal points that are at a very small distance to each other. This leads to the disappearance of these points, resulting in a reconnection of the adjacent elements. We therefore will call this the reconnection process.

The cutting process, by cutting previous larger elements into smaller pieces, removes these large elements, but also generates smaller elements. The reconnection process generates larger elements but removes those elements that are reconnected. We therefore have a random rearrangement of length scales in both directions.

The problem that has been considered in the companion paper, Wang and Peters [3] is a birth-and-death process which is continuous in time. The time rate of change of the number of grid cells between different classes of elements follows a Boltzmann-type evolution equation, cf. Van Kampen [4],

$$\frac{\partial}{\partial t}\big[n_x P_x(x,t)\big] = \int W(x|y) n_y P_y(y,t)\,\mathrm{d}y - \int W(y|x) n_x P_x(x,t)\,\mathrm{d}y \tag{5}$$

Here we have denoted by x the class under consideration, while y stands for the class from which transitions to x occur. Furthermore, $W(x|y)$ and $W(y|x)$ are the transition probability densities per unit time from y to x and from x to y, respectively.

The integrals in (5) represent the generation and removal of grid cells due to the cutting and reconnection processes. Since both these processes generate and remove grid points in class x there will be a total of four contributions to the rate of change of $P(x,t)$, where $P(x,t)$ stands for $P_l(l,t)$ namely:

(1) the generation by the cutting process (gc),
(2) the removal by the cutting process (rc),
(3) the generation by the reconnection process (gr),
(4) the removal by the reconnection process (rr).

A detailed discussion of these processes is given in Appendix A.

If there are small elements between intermediate extremal points as shown in Fig. 1, counting from left to right, for the 3rd full element bounded by the 3rd and the 4th extremal point, such elements will disappear as diffusion continues. Consequently, extremal points representing intermediate minima and maxima will drift towards each other. The element between them will drift in length scale space towards zero and disappear. This will be called the drift process.

The velocity of extremal points relative to each other is due to two contributions already described by Gibson [1]. For the linear elements that we are considering it scales as

$$v(x) = \frac{\mathrm{d}x}{\mathrm{d}t} = -\frac{4D}{x} \quad \text{for } x \to 0 \tag{6}$$

which is the velocity at which the very small elements drift to the origin (cf. Appendix B). This indicates that $v(x)$ is negative for small elements but must change sign and become positive for larger elements. In order to account for this, we introduce the ansatz

$$v(x) = -\frac{4D}{x}\big(1 - c\rho x \exp(-\rho x)\big) \tag{7}$$

The form of the exponential function in this ansatz was chosen to agree with velocity data from the 1D simulations shown below. Note that v is singular at the origin. This singularity requires $P(x,t)$ to be proportional to x at the origin.

Since the ensemble of elements must conserve the total length L we have the additional condition

$$\frac{\mathrm{d}L}{\mathrm{d}t} = \int_0^\infty v(x)\,P(x)\,\mathrm{d}x = 0 \tag{8}$$

Since the reconnection process is caused by the disappearance of the very small elements at the origin $x = 0$ the reconnection rate μ must be associated with this disappearance. During a small time span Δt elements of the classes $0 < x < \Delta x$ drift to the origin and disappear there such that, by integration of (6), Δx is related to Δt by

$$(\Delta x)^2 = 8D\Delta t \tag{9}$$

The number of small elements disappearing in the limit $\Delta x \to 0$ is

$$\int_0^{\Delta x} P(x)\,\mathrm{d}x = \int_0^{\Delta x} x\frac{\partial P}{\partial x}\bigg|_{x=0}\mathrm{d}x = \frac{(\Delta x)^2}{2}\frac{\partial P}{\partial x}\bigg|_{x=0} \tag{10}$$

since $P(0) = 0$. This number is proportional to the reconnection rate μ times the time span Δt, namely $\mu\Delta t$. With (9) and (10) this leads to

$$\mu = 4D\frac{\partial P}{\partial x}\bigg|_{x=0} \tag{11}$$

Using this and adding the drift term due to diffusion $v(x)$ to (A.13) one obtains after normalization of $v(x)$, $P(x,t)$ and x, y and z according to

$$\tilde{t} = t/(\rho^2 D), \qquad \tilde{x} = \rho x, \qquad \tilde{y} = \rho y, \qquad \tilde{z} = \rho z, \qquad \tilde{v}(\tilde{x}) = v(x)/(\rho D), \qquad \tilde{P}(\tilde{x},t) = P(x,t)/\rho \tag{12}$$

the non-dimensional equation, cf. Wang and Peters [3],

$$\frac{\partial \tilde{P}(\tilde{x},\tilde{t})}{\partial \tilde{t}} + \frac{\partial[\tilde{v}(\tilde{x})P(\tilde{x},\tilde{t})]}{\partial \tilde{x}} = \Lambda\left[2\int_{\tilde{x}}^{\infty} \tilde{P}(\tilde{y},\tilde{t})\,\mathrm{d}\tilde{y} - \tilde{x}\,\tilde{P}(\tilde{x},t)\right] + 8\frac{\partial \tilde{P}}{\partial \tilde{x}}\bigg|_{\tilde{x}\to 0}\left[\int_0^{\tilde{x}} \frac{\tilde{y}}{\tilde{x}}\,\tilde{P}(\tilde{x}-\tilde{y},t)\,\tilde{P}(\tilde{y},t)\,\mathrm{d}\tilde{y} - \tilde{P}(\tilde{x},t)\right] \tag{13}$$

Here Λ is a Peclet number defined by

$$\Lambda = \frac{\lambda}{\rho^3 D} \tag{14}$$

Eq. (13) must satisfy the normalization condition

$$\int_0^{\infty} \tilde{P}(\tilde{x},t)\,\mathrm{d}x = 1 \tag{15}$$

We will be looking for a steady state solution for $\tilde{t}\to\infty$ where it also must satisfy the condition that the mean value of the normalized variable $\tilde{x}$ should be unity

$$\int_0^{\infty} \tilde{x}\,\tilde{P}(\tilde{x})\,\mathrm{d}x = 1 \tag{16}$$

In this case Λ determines the mean value $\langle x\rangle = \rho$.

The 1D steady state solution of (13) has been determined numerically by a finite difference method. An unsteady solution method was applied for a chosen value of Λ, which converged to a steady state by applying the normalization condition at each time step. The value of Λ was then varied until (16) was satisfied.

The coefficient c in the drift velocity ansatz (7) was determined as $c = 4.137$ from the condition that the weighted sum over all velocities must vanish for a fixed total length (cf. (8)). The Peclet number was determined as $\Lambda = 18.52$. The maximum of the pdf occurs at $\tilde{x} = 0.57$ with a value of 0.84.

4. A one-dimensional test case

We want to analyze the random cutting and reconnection process by the superposition of solutions of the one-dimensional diffusion equation

$$\frac{\partial \phi}{\partial t} - D\frac{\partial^2 \phi}{\partial x^2} = 0 \tag{17}$$

Gaussian profiles of the form

$$\phi(x,t) = \pm\frac{1}{\sqrt{2\pi Dt}}\exp\left(-\frac{(x-x_i)^2}{4Dt}\right) \tag{18}$$

satisfy this equation. We superimpose such profiles with a fixed elapsed time $t = t_0$ at discrete times $t_i = i\,\Delta t$ at equally distributed random positions x_i within the range $-L < x_i < +L$, where $L = 5000$, and with alternating $+$ and $-$ signs. We assume that the scalar continues to diffuse during a fixed life time t_l such that the entire solution is written as

$$\phi(x,t) = \sum_{i=0}^{N} \frac{(-1)^i}{\sqrt{2\pi Dt'}}\exp\left(-\frac{(x-x_i)^2}{Dt'}\right) \tag{19}$$

where $t' = t - t_i + t_0$. Each term is different from zero only if $0 < t - t_i < t_l$.

The series in (19) is evaluated for typically 100 000 profiles added until a steady state average of the scalar variance $\langle \phi'^2\rangle$ is reached. It is evident that Gaussian profiles of older age will have decayed to small values, while more recently

Table 1
Mean quantities calculated from 1D simulations with random additions of Gaussian profiles

Tableau 1
Quantités moyennes calculées à partir de simulations 1D avec l'addition de profils Gaussiens

λ	t_0	$\langle\phi'^2\rangle$	ρ	$\tilde{x}_{\max}$	τ_ϕ	Λ	Λ_τ	$x_0/\langle x\rangle$
Case a	0.001	0.954	0.314	0.460	0.335	3.23	121.20	0.01
$\lambda = 0.1$	0.00316	0.953	0.313	0.470	0.442	3.39	90.68	0.0174
$t_l = 10$	0.01	0.975	0.312	0.460	0.635	3.42	64.80	0.0308
	0.0316	0.928	0.305	0.480	1.13	3.64	37.60	0.0536
	0.1	0.887	0.287	0.490	2.083	4.23	23.96	0.091
	0.316	0.826	0.247	0.550	3.60	6.64	18.20	0.139
	1.0	0.73.	0.179	0.646	6.51	17.4	19.00	0.179
	3.16	0.585	0.117	0.720	12.80	64.0	22.68	0.207
Case b	0.001	1.990	0.390	0.450	0.2265	3.36	115.60	0.0123
$\lambda = 0.2$	0.00316	1.965	0.389	0.447	0.363	3.40	72.40	0.0218
$t_l = 10$	0.01	1.940	0.385	0.440	0.628	3.50	43.04	0.0385
	0.0316	1.880	0.372	0.446	1.114	3.88	25.84	0.0661
	0.1	1.812	0.342	0.480	2.01	5.00	16.98	0.108
	0.316	1.677	0.275	0.590	3.62	9.6	14.68	0.154
	1.0	1.469	0.184	0.720	6.64	32.0	17.80	0.184
	3.16	1.168	0.117	0.720	12.88	125.0	22.56	0.208
Case c	0.001	1.404	0.398	0.485	0.185	3.17	136.80	0.0126
$\lambda = 0.2$	0.00316	1.389	0.397	0.476	0.277	3.20	91.84	0.0223
$t_l = 5$	0.01	1.362	0.392	0.470	0.462	3.32	56.36	0.0392
	0.0316	1.315	0.380	0.475	0.805	3.64	34.44	0.0675
	0.1	1.237	0.350	0.490	1.44	4.66	22.68	0.111
	0.316	1.110	0.285	0.630	2.597	8.64	18.92	0.160
	1.0	0.924	0.195	0.750	4.90	27.0	21.36	0.195
	3.16	0.689	0.126	0.800	10.17	100.0	24.66	0.224

generated profiles will exhibit pronounced minima and maxima. Distances between minima and maxima points are readily calculated. An example of the scalar profile with these distances l_i was shown in Fig. 1.

Parameters of the simulations are therefore the frequency of additions $\lambda = 1/(\Delta t U)$ per unit length $U = 1$ the diffusion coefficient D, and the elapsed time t_0 of the initial Gaussian profiles and their life time t_l. The diffusion coefficient D can be absorbed into the times t, t_0, t_l and Δt without altering the final steady state solution. Therefore we set $D = 1$ without loss of generality. We also note that t_l and Δt should be of the same order of magnitude if we want to avoid a physically unrealistic accumulation of Gaussian profiles ($t_l \gg \Delta t$) or the occurrence of very few isolated profiles ($\Delta t \gg t_l$). Since t_l should take values between 5 and 10 for a reasonable change of width of the initial Gaussian profiles with time, λ should vary between 0.1 and 0.2 . We will present data for $\lambda = 0.1$ and $t_l = 10$ (case a), $\lambda = 0.2$ and $t_l = 10$ (case b) and $\lambda = 0.2$ and $t_l = 5$ (case c). The only remaining parameter then is the elapsed time t_0 of the initial profile. These results are shown in Table 1.

Fig. 7 shows for the reference case $\lambda = 0.2$, $t_l = 10$, $t_0 = 0.316$ the comparison between the normalized length scale distribution function obtained from the random addition of Gaussian profiles and the one obtained from the steady state solution of (13). The simulation underpredicts the theoretical pdf for $\tilde{x} < 0.4$ and overpredicts it for larger values. The maximum value for the simulation lies at $\tilde{x}_{\max} = 0.6$ which needs to be compared to $\tilde{x}_{\max} = 0.57$ for the theory. The average from Table 1 for the location of the maximum is around 0.53, however. For the reference case the maximum of the pdf is 0.84 for the theory and 0.9 for the calculation. This may be compared to the value of 0.92 for the maximum in Fig. 6 which there occurs at $l/l_m = 0.6$.

The inserted log-linear graph in Fig. 7 shows an exponential decay up to values of $\tilde{x} = 2.0$ which also agrees with the exponential decay in Fig. 6. The result that the simulations do not reproduce the theoretical pdf exactly. This may be explained by the fact that the random addition of Gaussian profiles and the subsequent calculation of element lengths is not identical with the cutting and reconnection process for which the theory was formulated. Calculations where Δt was considerably larger than t_l with very few isolated profiles were more representative of a Poisson process and also showed an exponential decay over a much larger range of $\tilde{x}$.

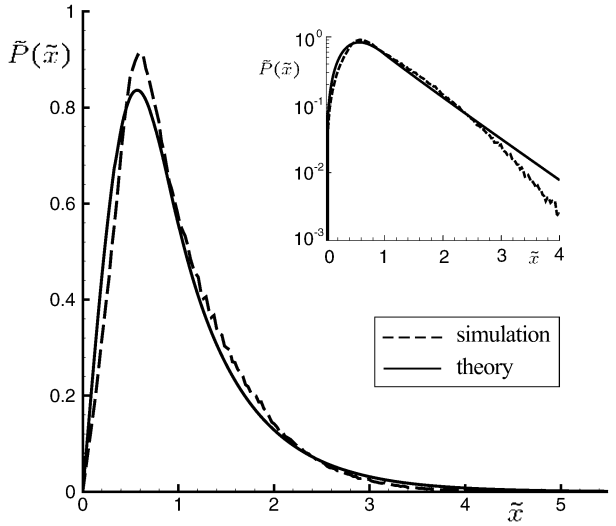

Fig. 7. Normalized length scale distribution from 1D simulations compared with the theoretical prediction.

Fig. 7. Distribution de l'échelle de longueur normalisée simulé en 1D comparée à la prédiction théorique.

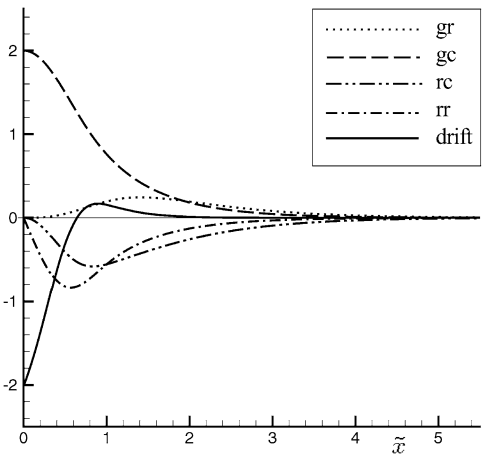

Fig. 8. Different terms in (13).

Fig. 8. Différents termes de (13).

It is interesting to compare the magnitude of the different terms in (13), as shown in Fig. 8. It turns out that generation by cutting (gc) process is the dominant production term for small elements $\tilde{x} < 2.0$. It is balanced by the drift term for $\tilde{x} < 0.5$ and by the two removal terms (rc) and (rr) for $0.5 < \tilde{x} < 1.5$. The generation by reconnection (gr) process generates larger elements but remains relatively small. Both removal terms (rc) and (rr) are negative everywhere, the former removing larger elements and the latter smaller elements as expected.

The conditional mean drift velocity for the reference case is shown in Fig. 9 and compared with the ansatz (7). While there is still a difference between the two curves both expressions tend to the limit $\tilde{v}(x) \to -4/\tilde{x}$ for small $\tilde{x}$ and become negative for larger values of $\tilde{x}$.

Fig. 10 shows the position of extremal points in part of the simulation domain as a function of time. One first notices the generation of pairs of extremal points which in many cases diffuse towards each other and then disappear. However, there also are many cases where lines associated with an extremal point suddenly disappear. Nearly all these cases are associated with the generation of other points in their close vicinity. This indicates that in these cases the addition of a Gaussian profile has altered the resulting scalar profile in such a way that previous extremal points are removed while new ones are created. The new elements between these extremal points therefore are local successors of those that have disappeared, with a sudden change of their length, leading to a jump in their drift velocity. On the other hand this also means that not every cutting process resulting from the addition of a Gaussian profile is successful. If the cutting occurs with relatively wide Gaussian profiles (t_0 large) as compared to the mean element length the cutting frequency will therefore cede to be a relevant parameter.

Apart from the diffusive time scale $t_D = 1/(\rho^2 D)$ there are two non-diffusive time scales in this problem, the time scale $t_\lambda = \rho/\lambda$ and an integral scalar time which we define as

$$\tau_\phi = \frac{\langle \phi'^2 \rangle}{4\chi} \tag{20}$$

where the variance $\langle \phi'^2 \rangle$ and the scalar dissipation rate $\chi = 2D\langle (\mathrm{d}\phi/\mathrm{d}x)^2 \rangle$ was obtained from averages of the simulated 1D profiles. The factor 4 in the denominator was motivated by the factor 4 in (6) which indicates that the effective diffusion coefficient for dissipative elements is four times larger than the nominal one.

The question arises which non-diffusive time scale is the relevant one to describe the effective cutting frequency. The scalar time was calculated for all cases and is given in Table 1. Two Peclet numbers where calculated from the simulations using the time scales $\tau_\lambda = \rho/\lambda$ and τ_ϕ, respectively, Λ defined being by (14) and Λ_τ by

$$\Lambda_\tau = (\rho^2 D \tau_\phi)^{-1} \tag{21}$$

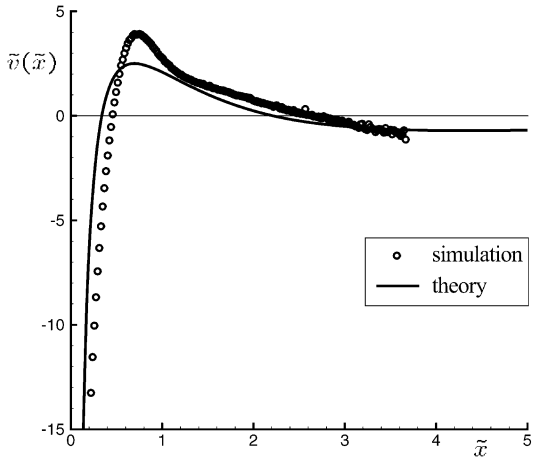

Fig. 9. The conditional mean drift velocity from the simulation compared with the ansatz used in the theory.

Fig. 9. Moyenne conditionnelle de la vitesse de dérive simulée comparée à l'ansatz utilisé dans la théorie.

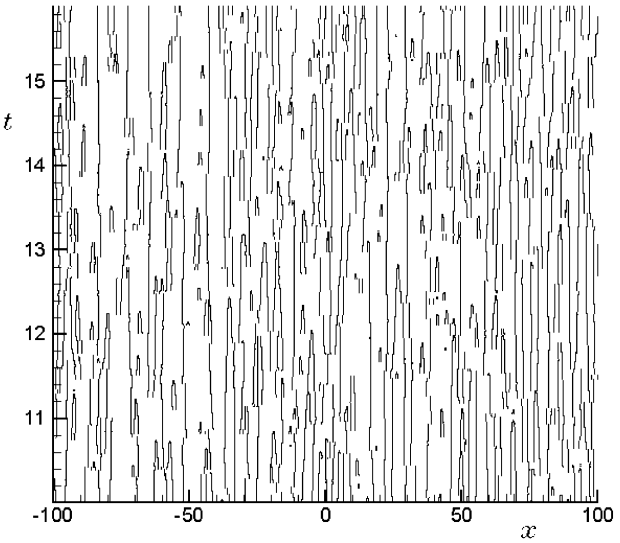

Fig. 10. The generation of extremal points and their disappearance by diffusion.

Fig. 10. Génération de points extrêmes et leur disparition par diffusion.

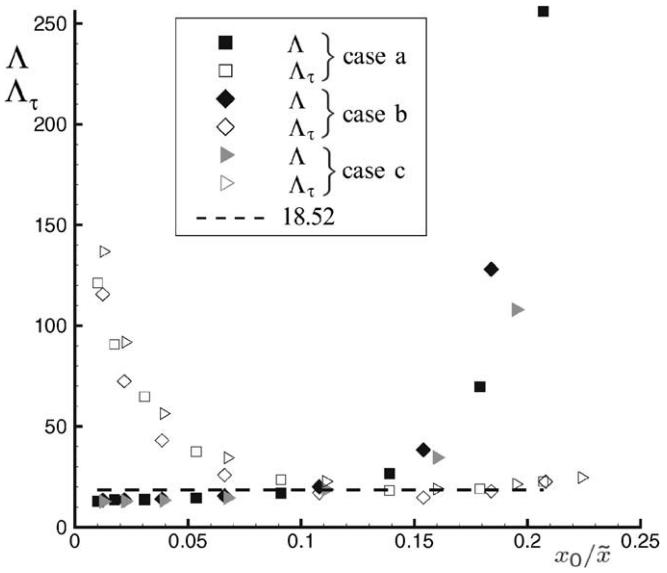

Fig. 11. Two different definitions for the Peclet number compared with the theoretical eigenvalue of 18.52.

Fig. 11. Deux définitions différentes pour le nombre de Peclet comparées à la valeur propre théorique de 18.52.

They are to be compared with the eigenvalue $\Lambda = 18.52$ obtained from the steady state solution of (13). The values for Λ and Λ_τ are given in Table 1 and are plotted over the length scale ratio

$$\frac{x_0}{\langle x \rangle} = (\rho^2 D t_0)^{1/2} \tag{22}$$

in Fig. 11. Here $x_0 = (Dt_0)^{1/2}$ is the characteristic width of the initial Gaussian profile at the elapsed time t_0. Fig. 11 shows that Λ is reasonably constant for small values of the length scale ratio but grows rapidly for larger values. This was to be expected after the observation of unsuccessful cuttings for large values of t_0 in Fig. 10. On the other hand

Λ_τ is large for small values of the length scale ratio but becomes nearly constant at larger values and close to the theoretical value of 18.52. Since Gaussian profiles with large values of t_0 are expected to model eddy turnover events better than profiles with pronounced minima and maxima we conclude that the simulations with a large length scale ratio are more relevant and that the effective cutting occurs with the integral scalar time scale τ_ϕ. We therefore set

$$\rho/\lambda = \tau_\phi \tag{23}$$

which is of the order of the integral time scale $\tau = k/\varepsilon$. Inserted into (14) this scaling leads with $\rho = l_m^{-1}$ to an important conclusion, namely that the mean element length

$$l_m \sim (D\tau)^{1/2} \sim (\nu k/\varepsilon)^{1/2} \sim \lambda \tag{24}$$

is proportional to the Taylor scale λ. This is expected to be valid for 3D as well.

5. Conclusions

Dissipation elements for passive scalar turbulence obtained from DNS data from homogeneous shear flow display a length scale distribution function similar to that obtained from a theory based on a stochastic evolution equation. The predicted pdf was tested against 1D simulations of the random cutting and removal process which was hypothesized to mimic the generation and disappearance of minimum and maximum points. There is a good agreement between the length distribution from the 3D DNS, the 1D simulations and the theoretical shape, both as far as the predicted exponential tail and the location and the value of the maximum of the pdf are concerned. The exponential tail in the DNS results seems to justify the random Poisson process which was used in the theory and in the 1D simulations for the generation of extremal points. The frequency of generating extremal points seems to scale with the integral scalar time scale rather than with a shorter time such as the Kolmogorov time as one might have expected. This is due to the inefficiency of this process because it also destroys previous elements while it is generating new dissipation elements. It is concluded that the mean length scale of the distribution function is of the order of the Taylor scale.

Acknowledgements

The authors acknowledge the funding of this work by the Deutsche Forschungsgemeinschaft under Grant Pe 241/30-1. They have greatly benefited from interactions with colleagues, and are particularly grateful for those with Carl Gibson, Heinz Pitsch, Martin Oberlack, Rupert Klein, Chenning Tong, Sutanu Sarkar and Parviz Moin.

Appendix A. Derivation of the four contributions to the evolution equation

For the cutting process we first consider the generation (gc) of grid cells in the class of smaller elements of size x from those of a larger element of size y. The time rate of change due to this process is therefore

$$\frac{\partial}{\partial t}[n_x P_x]_{\mathrm{gc}} = \int_x^\infty W_{\mathrm{gc}}(x|y) n_y P_y(y,t)\,\mathrm{d}y \tag{A.1}$$

After some detailed considerations outlined in Wang and Peters [3] we obtain for the transition probability density of the cutting process (gc)

$$W_{\mathrm{gc}}(x|y) = 2\lambda\frac{x}{y} \tag{A.2}$$

where λ is the effective cutting frequency per unit length.

Next we consider the removal (rc) of grid cells by cutting an element of class x to smaller elements of other classes. The time rate of change of $n_x P_x$ due to this process is

$$\frac{\partial}{\partial t}[n_x P_x]_{\mathrm{rc}} = -n_x P_x \int_0^x W_{\mathrm{rc}}(y|x)\,\mathrm{d}y \tag{A.3}$$

where

$$W_{\mathrm{rc}}(y|x) = \lambda x P_{x\to y} \tag{A.4}$$

The probability density of transitions $P_{x\to y}$ will be independent of y and uniform in $0 \leqslant y \leqslant x$ with the normalization condition

$$\int_0^x P_{x\to y}\,\mathrm{d}y = 1 \tag{A.5}$$

Therefore the time rate of change of the (rc) process becomes

$$\frac{\partial}{\partial t}[n_x P_x]_{\mathrm{rc}} = -\lambda x n_x P_x \tag{A.6}$$

The generation by the reconnection process (gr) is due to the generation of larger elements of class x from a smaller element of class y when extremal points are removed by the disappearance of very small elements. In Fig. 1 the smallest element would disappear by diffusion, thereby reconnecting their nearest neighbors. The time rate of change of $n_x P_x$ due to this process is

$$\frac{\partial}{\partial t}[n_x P_x]_{\mathrm{gr}} = \int_0^x W_{\mathrm{gr}}(x|y) n_y P(y,t)\,\mathrm{d}y \tag{A.7}$$

Since elements of class y cannot become larger than those of the fixed class x the integration is performed between 0 and x.

The two extremal points of the very small elements become a single point when the reconnection occurs. Attached to the two extremal points are two adjacent elements. We will denote the rate of reconnection at each extremal point by μ. Therefore the transition probability density per unit time of this process is

$$W_{\mathrm{gr}}(x|y) = 2\mu P_{y\to x}(x,y) \tag{A.8}$$

The probability density $P_{y\to x}$ is equal to

$$P_{y\to x} = P_z(x-y,t) \tag{A.9}$$

where $z = x - y$ is the class of elements that combines with an element of class y to form an element of class x. We therefore obtain for the time rate of change due to the (gr) process

$$\frac{\partial}{\partial t}[n_x P_x]_{\mathrm{gr}} = 2\mu \int_0^x P_z(x-y,t) n_y P_y(y,t)\,\mathrm{d}y \tag{A.10}$$

It may be noted that, apart from the factor n_y, the integral on the r.h.s. is the convolution of the statistically independent densities $P_y(y)$ and $P_z(z)$ resulting in the density $P_x(x)$ that one obtains for the addition of random variables y and z according to $y + z = x$.

Finally, the time rate of change of $n_x P_x$ by the removal of one of the 2 smaller elements of class x by the reconnection process (rr) is

$$\frac{\partial}{\partial t}[n_x P_x]_{\mathrm{rr}} = -2\mu n_x P_x \tag{A.11}$$

following similar arguments as those that led to (A.13)

Since the probability densities of the three classes of elements x, y and z are equal to each other we will introduce the notation $P(x,t)$ without index

$$P_x(x,t) = P_y(y,t) = P_z(z,t) \equiv P(x,t) \tag{A.12}$$

Furthermore, the number of grid cells n_x and n_y within the elements are proportional to x and y, respectively, for a uniform mesh. Since the proportionality factors cancel when n_x and n_y are inserted into the terms of (5) one obtains after division by x for the time rate of change of the probability density $P(x,t)$ itself

$$\frac{\partial P(x,t)}{\partial t} = 2\lambda \int_x^\infty P(y,t)\,\mathrm{d}z - \lambda x P(x,t) + 2\mu \int_0^x \frac{y}{x} P(x-y,t) P(y,t)\,\mathrm{d}y - 2\mu P(x,t) \tag{A.13}$$

The steady state solution of this equation should yield the exponential distribution describing the probability density of the distance between two Poisson points along a line (Papoulis [5, p. 355])

$$P(x) = \rho \exp(-\rho x) \tag{A.14}$$

where $\rho = 1/\langle x\rangle$ is the mean number of elements per unit length with $\langle x\rangle$ being the average length of elements. For the steady state Poisson process the rates of additions and the rates of removals of Poisson points per unit length are equal

$$\lambda = \mu\rho \tag{A.15}$$

It is easily verified that with this (A.14) satisfies the steady state form of (A.13). Note that in this case the (gc) term balances the (rr) term and the (gr) term the (rc) term thereby creating a cross link between the cutting and the reconnection process.

Appendix B. Calculation of the drift velocity

Generally, for any scalar field $z(\mathbf{x},t)$), the scalar values at extremal points can be expressed as $z(\mathbf{x}_0(t),t)$, where $\mathbf{x}_0(t)$ is the time-dependent location vector of the extremal point. For extremal points, the zero gradient condition should be satisfied:

$$\nabla z|_{\mathbf{x}=\mathbf{x}_0(t)} = \mathbf{0} \tag{B.1}$$

This condition holds for all times

$$\frac{\partial}{\partial t}(\nabla z|_{\mathbf{x}=\mathbf{x}_0(t)}) = \nabla\left(\left.\frac{\partial z}{\partial t}\right|_{\mathbf{x}=\mathbf{x}_0}\right) = \mathbf{0} \tag{B.2}$$

The time derivative of z moving with the extremal point may be written as

$$\left.\frac{\partial z}{\partial t}\right|_{\mathbf{x}=\mathbf{x}_0} = \frac{\partial z}{\partial t} + \nabla z \cdot \left.\frac{\partial \mathbf{x}}{\partial t}\right|_{\mathbf{x}=\mathbf{x}_0} \tag{B.3}$$

where $\partial z/\partial t$ is the local time derivative and $\partial\mathbf{x}/\partial t|_{\mathbf{x}=\mathbf{x}_0}$ is the displacement speed of the extremal point $\mathbf{x}_0$. Taking the gradient of (B.3) as in the second equality of (B.2) one obtains

$$\frac{\partial}{\partial t}(\nabla z) + \nabla^2 z \left.\frac{\partial \mathbf{x}}{\partial t}\right|_{\mathbf{x}=\mathbf{x}_0} = \mathbf{0} \tag{B.4}$$

The displacement speed of the extremal point can therefore be expressed in terms of local derivatives

$$\left.\frac{\partial \mathbf{x}}{\partial t}\right|_{\mathbf{x}=\mathbf{x}_0} = -\frac{\frac{\partial}{\partial t}(\nabla z)}{\nabla^2 z} \tag{B.5}$$

For the 1D case, (B.5) simplifies to

$$\left.\frac{\partial x}{\partial t}\right|_{x=x_0} = \frac{\frac{\partial^2}{\partial t^2}(\nabla z)}{\frac{\partial^2 z}{\partial x^2}} \tag{B.6}$$

For very small 1D elements governed by the diffusion Eq. (17) the scalar can locally be expanded around the mid point with $z(0,t) = 0$ for small x into a harmonic function

$$z(x,t) = \sum_{i=1}^{\infty} \exp\left(-\frac{Dt}{(il_0)^2}\right) \sin\left(\frac{x}{il_0}\right) \tag{B.7}$$

Using (B.6) and the diffusion equation (17) the displacement speed of extremal points is for this case

$$\left.\frac{\partial x}{\partial t}\right|_{x=x_0} = -D\frac{\partial^3 z/\partial x^3}{\partial^2 z/\partial x^2} \tag{B.8}$$

With (B.7) this can be evaluated for small $x = x_0$ as

$$\left.\frac{\partial x}{\partial t}\right|_{x=x_0} = -\frac{D}{x_0} \tag{B.9}$$

using the condition that $\sin(x_0/l_0) \approx x_0/l_0$ as x_0 tends to zero.

The drift velocity of a symmetric small element is two times the drift velocity of extremal points and the length of the element is $l = 2x_0$. Therefore the drift velocity is

$$v(l) = -2\frac{D}{x_0} = -4\frac{D}{l} \tag{B.10}$$

References

[1] C.H. Gibson, Fine structure of scalar fields mixed by turbulence I. Zero gradient points and minimal gradient surfaces, Phys. Fluids 11 (1968) 2305–2315.
[2] S. Sarkar, The stabilizing effect of compressibility in turbulent shear flow, J. Fluid Mech. 282 (1995) 163–186.
[3] L. Wang, N. Peters, The length scale distribution function of the distance between extremal points in passive scalar turbulence, J. Fluid Mech. 554 (2005) 457–475.
[4] N.G. Van Kampen, Stochastic Processes in Physics and Chemistry, Elsevier, 1992.
[5] A. Papoulis, Probability, Random Variables and Stochastic Processes, third ed., McGraw-Hill Inc., 1991.